ELSEVIER

Chemical Engineering Journal 73 (1999) 247–253

Chemical Engineering Journal

Short communication

Heat transfer in the drag reducing regime of wood pulp fibre suspensions

Md. Salim Newaz Kazi, Geoffrey G. Duffy*, Xiao Dong Chen[1]

Department of Chemical and Materials Engineering, School of Engineering, The University of Auckland, Private Bag 92019, Auckland, New Zealand

Received 22 August 1998; received in revised form 17 December 1998; accepted 17 December 1998

Abstract

Heat transfer to suspensions of different grades of wood pulp fibres at different concentrations were investigated over a range of flow rates. It was observed that a small amount of fibre in suspension causes drag reduction and reduces the heat transfer coefficient below that for water. Both effects are a function of concentration, flow rate and fibre type. The more flexible fibres produce a greater level of drag reduction and a greater lowering of heat transfer coefficient. The measurement of heat transfer coefficient provides a method of comparing fibres of different flexibility for papermaking. © 1999 Elsevier Science S.A. All rights reserved.

Keywords: Fibres; Wood pulp; Fibre suspensions; Flocculation; Viscoelastic suspensions; Drag reduction; Heat transfer; Heat transfer coefficient

1. Introduction

Neighbouring fibres in suspension interact and entangle even at low populations and can form bundles or entities that behave differently from the individual fibres. Fibres interlock at moderate concentrations to form three-dimensional structures or networks which in liquid suspension alter the transport properties of the suspension. Several mechanisms of fibre suspension flow have been investigated and identified [1]. Wood pulp fibres form flocs and coherent networks which in a pipe produce a plug occupying the entire pipe volume. At low flow velocities the frictional resistance is greater than for water alone but at higher velocities, fibres pulled from the network damp turbulence and reduce the frictional drag below that for water (drag reduction). In the transition region between plug flow and fully developed turbulence, fibres, floc fragments, and a network core coexist and, hence, the transfer of momentum is complicated by both 'particle' and floc behaviour and the presence of a central coherent fibre plug. In the transition flow regime the momentum transfer is enhanced by the interlocking fibres behaving as a solid continuum. However, fibres and flocs damp turbulent eddies which tend to reduce the effective momentum transfer. Momentum transfer enhancement, therefore, predominates at low flow rates and the fibre damping mechanism is controlling at higher velocities [2]. This competitive process results in a maximum level of drag reduction at an intermediate flow rate.

Momentum transfer and heat transfer are interrelated in conventional fluid flow [3] and it would be expected that fibre suspensions would alter both the mechanisms and rates of transfer. At low flow rates the annular layer between the plug and the wall is thin, whereas at high flow rates the individual fibres and neighbouring flocs modify eddy formation and dissipation near the wall. These phenomena would also affect the rate of heat transfer. The work reported in this paper provides a basis for further investigations and some insights into the mechanisms of heat and momentum transfer in fibre suspension flows.

2. Experimental

2.1. Flow loop

A diagram of the test flow loop is presented in Fig. 1. The flow loop consists of a tank, variable speed pump, magnetic flowmeter, heated pipe section, heat exchanger for cooling both inside the tank and in the flow loop, and a recycle piping system. The pump is an Allis–Chalmers PWO open-impeller centrifugal pump driven by a 20 kW AC motor controlled by a Plessy variable speed AC controller. Flow is measured with a 50 mm ABB Kent-Taylor (MagMaster) flow meter calibrated in the range of 0–20 l/s.

The suspension is pumped through PVC piping to the heat transfer test section and then through a double-pipe heat

*Corresponding author. E-mail: gg.duffy@aukland.ac.nz

[1]Co-corresponding author.

1385-8947/99/$ – see front matter © 1999 Elsevier Science S.A. All rights reserved.
PII: S1385-8947(99)00047-9

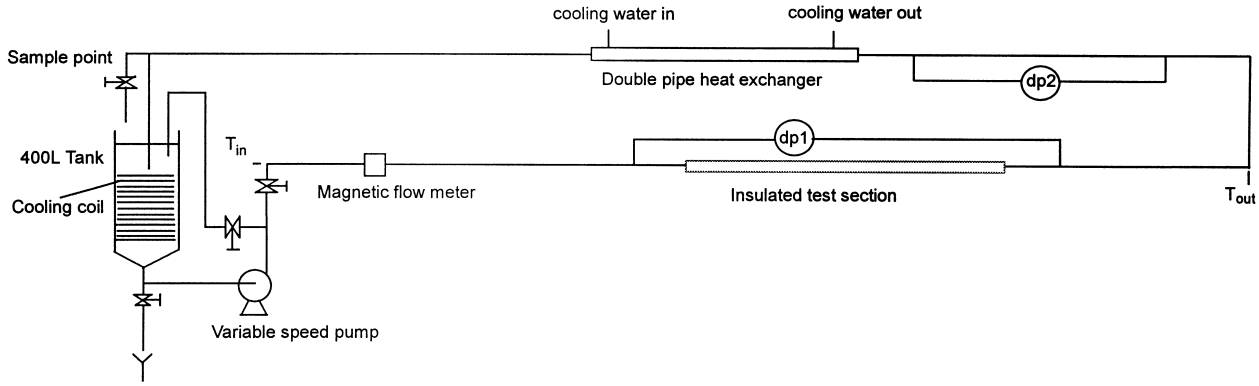

Fig. 1. Schematic diagram of experimental flow loop.

exchanger for first stage cooling before returning to the 400 l tank via a submerged pipe. It is cooled further to the desired temperature by a submerged cooling coil. Inlet and outlet bulk temperatures to the test section are measured with Type-K thermocouples located in the centre of the flow. The thermocouples are inserted facing downstream in the elbows before and after the test section to reduce fibre stapling.

2.2. Heat transfer test section

The heat transfer test section is made from smooth 316 L stainless steel pipe (Cr/Ni low-carbon stainless steel). The heat source consists of 10 Watlow band heaters clamped on the outside of the pipe. Four Type-E thermocouples are embedded in the pipe wall near the inside surface to obtain the wall temperature at a point approximately 110 mm in from the discharge end of the heated section. Two sets of pressure tappings, one across the test section and the other at the plastic pipe at downstream return line are connected to Kent differential pressure transducers to obtain friction loss measurements. The significant dimensions of the heat transfer test section are: length 646 mm, inside diameter 49.25 mm, hydrodynamic entry length 3.21 m (65 diam) and thermal entry length 536 mm (10.9 diam).

2.3. Experimental procedure

Different grades of bleached kraft *Pinus Radiata* pulp, from New Zealand Forest Products, were used in these experiments. The pulp sheets were soaked for a minimum of 18 h before being dispersed in water while the flow system was on recycle. The fibres were recycled for 30 min to disperse them completely. For each investigation the bulk velocity was measured in the range from 0.6–8 m/s while temperature measurements were obtained from the thermocouples located in the wall and in the centre of the flow.

Pulp samples were taken at the beginning and end of each run to obtain pulp concentrations. The samples were weighed, filtered, dried and reweighed and the concentration reported as the percentage dry fibre mass per mass of total suspension.

2.4. Data processing

Data for pressure drop, inlet and outlet temperatures, wall temperature, heater power input, and flow rate, were logged using a Hewlett Packard data acquisition system and recorded in a digital computer. The energy input to the heater per unit surface area was calculated as a heat flux q, being the total power input divided by the heated area A. The heater wall temperature T_w was calculated from the thermocouple values T_{tc} in the test section with a correlation to account for the distance of the thermocouples from the inner pipe surface. Details of the accurate determination of wall temperature using the Wilson plot method are given by Epstein [4]. The correction factor (wall resistance) is the ratio of the distance x of the thermocouple below the surface, to the wall thermal conductivity λ. The temperature difference between the thermocouple embedded in the wall and the actual surface temperature is, therefore, given by the product of heat flux and wall resistance x/λ

$$T_w = \frac{T_{tc} - q}{\lambda/x} \tag{1}$$

The local heat transfer coefficient α was determined from the calculated wall temperature T_w, the bulk temperature T_b and the heat flux q

$$\alpha = \frac{q}{T_w - T_b} \tag{2}$$

The bulk temperature T_b is the position-weighted average value of the inlet and outlet temperatures.

The values of friction factor f were calculated from the pressure drop per unit length $\Delta P/L$, bulk velocity V, pipe diameter D, and suspension density ρ

$$f = \left(\frac{\Delta P}{L}\right)\left(\frac{D}{2\rho V^2}\right) \tag{3}$$

The j-factor for heat transfer j_H was calculated from

Nusselt number (Nu), Reynolds number (Re) and Prandtl number (Pr)

$$j_H = Nu\,Re^{-1}Pr^{-1/3} \tag{4}$$

3. Result and discussion

3.1. Calibration of test loop with water

The test loop was calibrated with water and friction loss and heat transfer measurements were compared with published correlations. In addition, the average values of the thermal resistance x/λ were obtained for the four embedded thermocouples.

All experiments were performed at a constant temperature-difference between the wall and the liquid of 5°C to minimize the effect of changes in liquid physical properties with temperature. Values of heat transfer coefficient were determined from actual thermocouple temperatures T_{tc} and plotted as a function of velocity to determine the thermal wall resistance. The graph of reciprocal heat transfer coefficient versus V^n is known as a Wilson plot [5]. Epstein [4] found that the slope n was more accurately determined by non-linear regression analysis of the data. The intercept of the extrapolated curves on the y-axis is the thermal wall resistance used in Eq. (1).

Heat transfer and pressure drop measurements for water were obtained for a wide range of flow velocities at a constant bulk temperature. Graphs of friction factor (Fanning) f versus Re, and heat transfer coefficient α versus Re, are presented in Figs. 2 and 3. Friction factor data correlations obtained from measurements over two different lengths of pipe agreed well with the Colebrook and White correlation (including the effect of roughness) [6], except at the lowest flow rates where accurate pressure differential measurements are difficult to obtain

$$\frac{1}{\sqrt{f}} = 3.48 - 1.7372\left[\ln\left(\frac{\varepsilon}{r} + \frac{9.35}{Re\sqrt{f}}\right)\right] \tag{5}$$

where r is the radius of the circular duct and ε is the roughness height. Good agreement was obtained between the experimental and theoretical results when a relative roughness ratio ε/r of 0.0012 was used.

The values of heat transfer coefficient were compared with those obtained from the correlation of Martinelli [7] for fully developed turbulent flow in the fully rough flow regime of a circular duct

$$Nu = \frac{RePr\sqrt{f/2}}{5\left[Pr + \ln(1+5Pr) + 0.5\ln\left(Re\sqrt{f/2}/60\right)\right]} \tag{6}$$

The experimental data agreed well (Fig. 3) with values predicted by the Martinelli equation both at specified low and high Reynolds numbers.

3.2. Pulp flow friction loss measurements

Typical friction loss data obtained in this investigation are plotted in Fig. 4 as normalised drag reduction ratio versus bulk velocity. Drag reduction ratio is defined as the ratio of the pressure drop of the fibre suspension to the pressure drop for water alone at the same flow rate and applies in the transition flow regime between plug and fully developed turbulent flow. The data presented in this form are similar to those obtained previously [8]. Drag reduction ratio is actually greater than unity at low flow rates (plug flow regime), mainly due to the presence of a plug where the turbulent sheared layer between the plug and the pipe wall is very thin and the velocity profile steep [9]. Drag reduction ratio is lower than unity at high flow rates because fibres damp turbulence in this regime. Both the onset of drag reduction

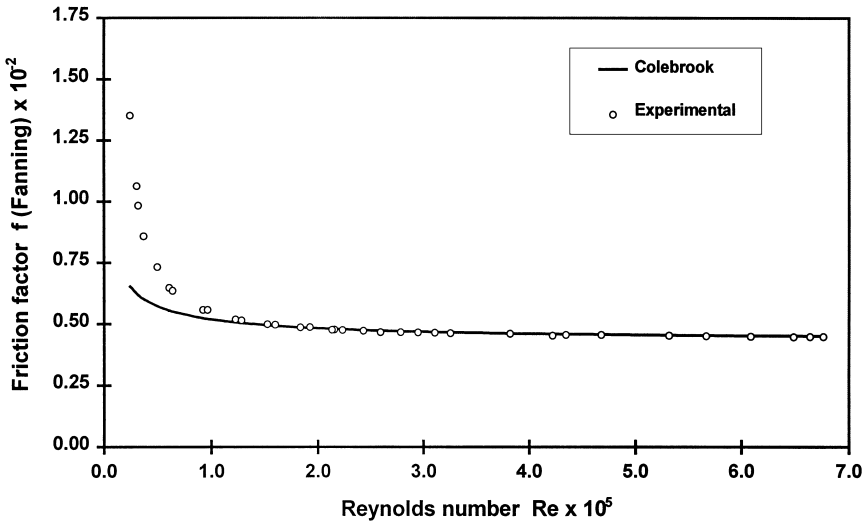

Fig. 2. Friction factor versus Reynolds number for water. Bulk temperature at 30°C and surface to bulk temperature difference as 5°C.

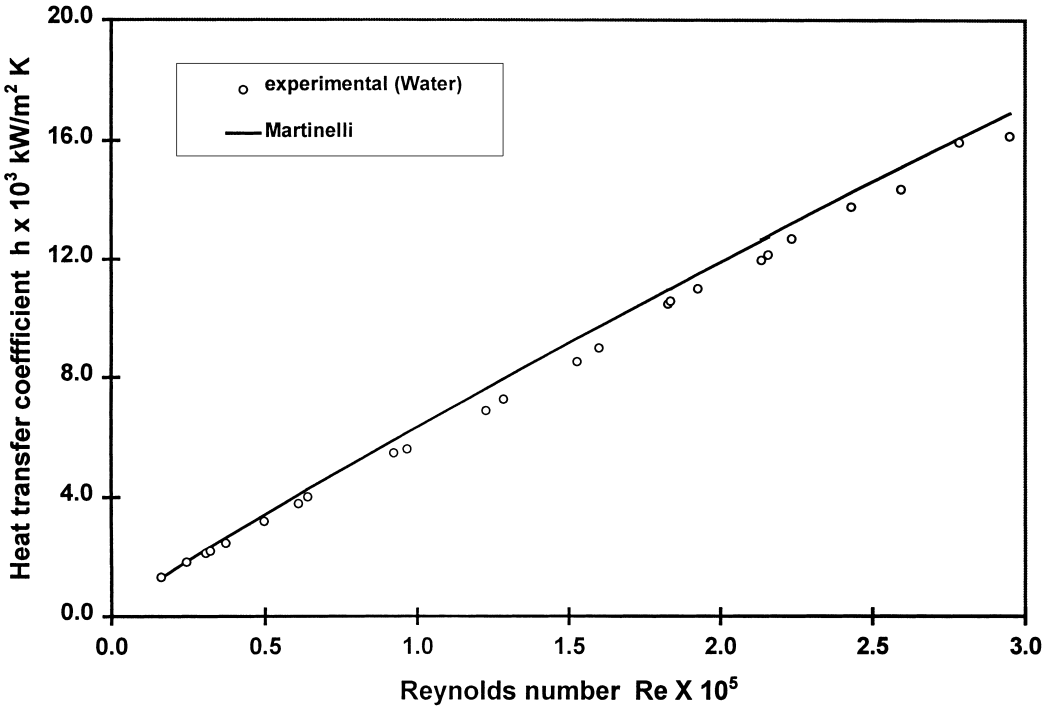

Fig. 3. Heat transfer coefficient versus Reynolds number for water. Bulk temperature at 30°C and surface to bulk temperature difference as 5°C.

and the point of maximum drag reduction are shifted to higher velocities with increasing fibre concentration due to the increased network strength of the fibre network. This trend in the results is in agreement with previous investigations [2]. Beyond the point of maximum drag reduction, the curves increase and level out at a value of approximately unity, indicating that fibre suspensions behave like water line at very high flow rates.

3.3. Pulp flow-heat transfer measurements

Heat transfer data for the same fibre at the same concentrations (0.5 and 0.8%) are presented in Fig. 5 and compared with the Martinelli correlation for water. These data are also presented in Fig. 6 as heat transfer coefficient ratio versus velocity for comparison with the drag reduction ratio data of Fig. 4. At low flow rates the heat transfer

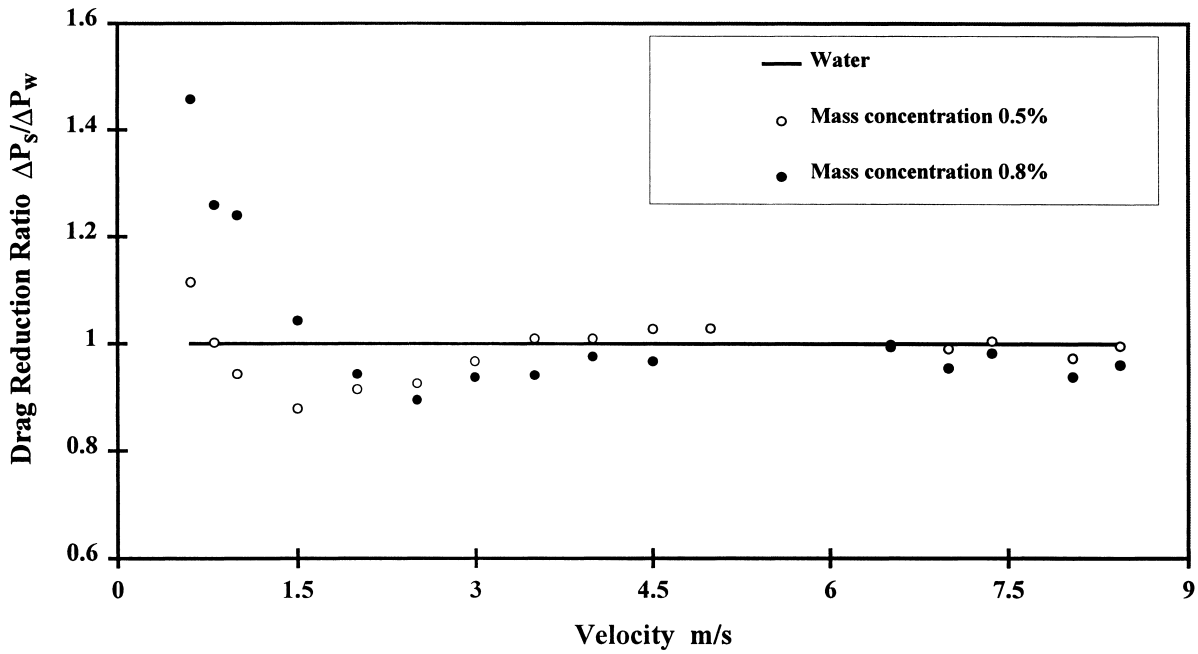

Fig. 4. Drag reduction ratio for a fibre suspension as a function of velocity at bulk temperature of 30°C and surface to bulk temperature difference as 5°C.

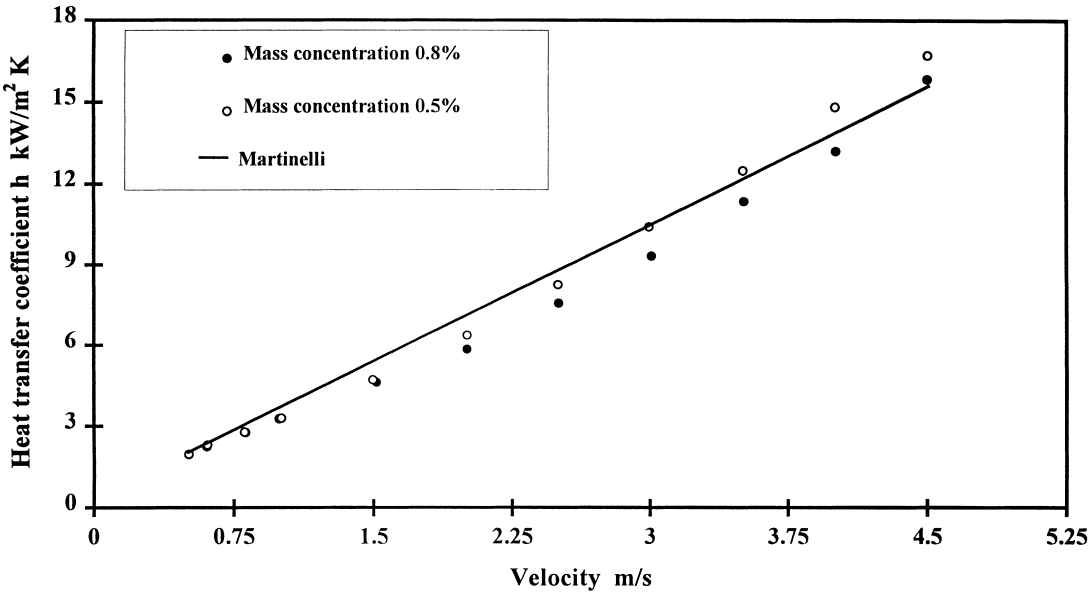

Fig. 5. Heat transfer coefficient versus velocity for water and fibre suspensions of different mass concentration. Bulk temperature at 30°C and surface to bulk temperature difference as 5°C.

coefficient ratio is not greater than unity (as for the case of Drag Reduction Ratio). However, similar trends in the curves are observed at higher flow rates with minima in the curves at intermediate flow rates and the curves approaching unity at higher flow rates. In addition, the initial decrease in heat transfer coefficient ratio occurs at much lower velocities than at the onset of drag reduction and the subsequent initial decrease in drag reduction ratio.

Fig. 7 is a plot of the j factor as a function of Reynolds number Re for both water and two concentrations of pulp suspension. The results for water agree with previous investigators for long smooth pipes [10]. Fibre suspensions are different from water as the curves are below the water curve and clearly exhibit minima in j_H caused by the drag reduction and heat transfer coefficient reduction.

3.4. Effect of fibre flexibility on heat transfer and drag reduction

Plots of drag reduction ratio and heat transfer coefficient ratio versus flow velocity have been obtained for several different types of fibres derived from the one wood resource *Pinus Radiata*. Typical data are presented in Figs. 8 and 9 for two different grades of bleached fibre at the same fibre

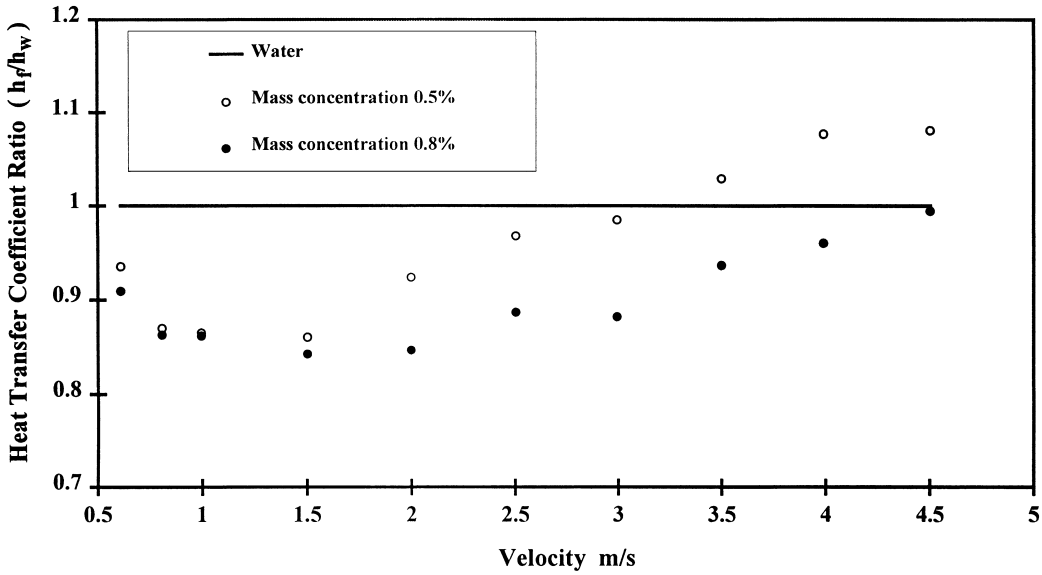

Fig. 6. Heat transfer coefficient ratio for a fibre suspension (Bleached Kraft) in water and water as a function of velocity. Bulk temperature 30°C and surface to bulk temperature difference as 5°C.

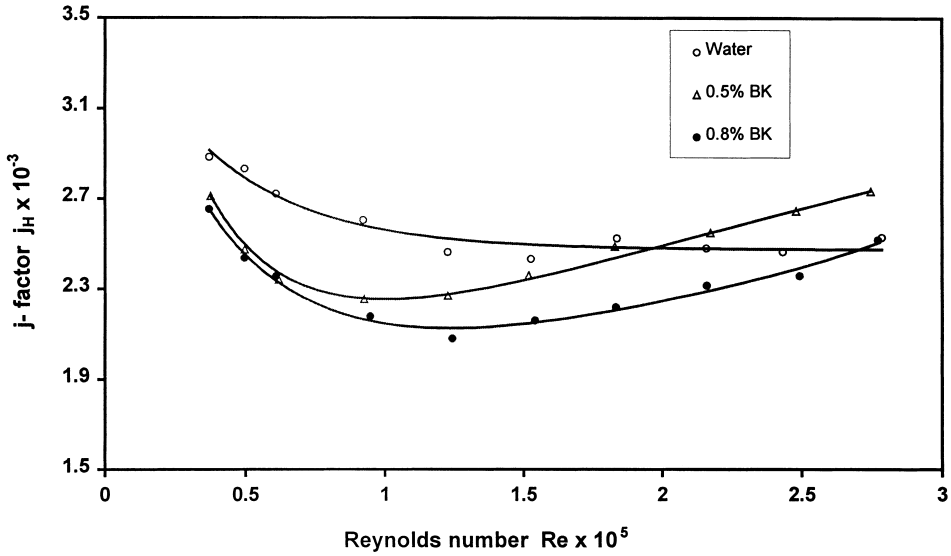

Fig. 7. *j*-factor for heat transfer j_H for fibre suspension (Bleached Kraft) in water versus Reynolds number. Bulk temperature at 30°C and surface to bulk temperature difference as 5°C.

concentration. Wood pulp fibres are hollow cylindrical elements which have varying cell wall thickness values. Stiffer fibres have thicker cell walls and a higher value of coarseness (higher mass/unit length) than the thin-walled, lower coarseness fibres. The thinner walled fibres are, therefore, more flexible and would be expected to modify the turbulent eddies to a greater extent than the stiffer, coarser fibres. It can be noted in Fig. 9 that the more flexible fibres (ultra low coarseness) reduce the heat transfer coefficient to a greater extent. At 1.5 m/s the ratio is 0.78 for flexible fibres and 0.84 for less flexible fibres. At about 3 m/s the ratio is 0.86 for flexible fibres (heat transfer coefficient of 9.2 kW/m^2) and 0.94 for high coarseness fibres (10 kW/m^2). Hence, the heat transfer coefficient could provide a means of monitoring fibre flexibility in papermaking. The graphs of drag reduction ratio versus flow velocity (Fig. 8) also show increased drag reduction with the increasing fibre flexibility but the differences are smaller and appear not to be as systematic due to difficulties in measuring pressure differentials accurately.

4. Conclusions

Heat transfer coefficient is a function of fibre concentration, fibre type and bulk velocity. Fibres damp turbulence at low suspension concentrations and, therefore, reduce the heat transfer coefficient. Drag reduction also occurs even at low fibre concentrations. Drag reduction increases and heat transfer coefficient decreases with the increase of flexibility

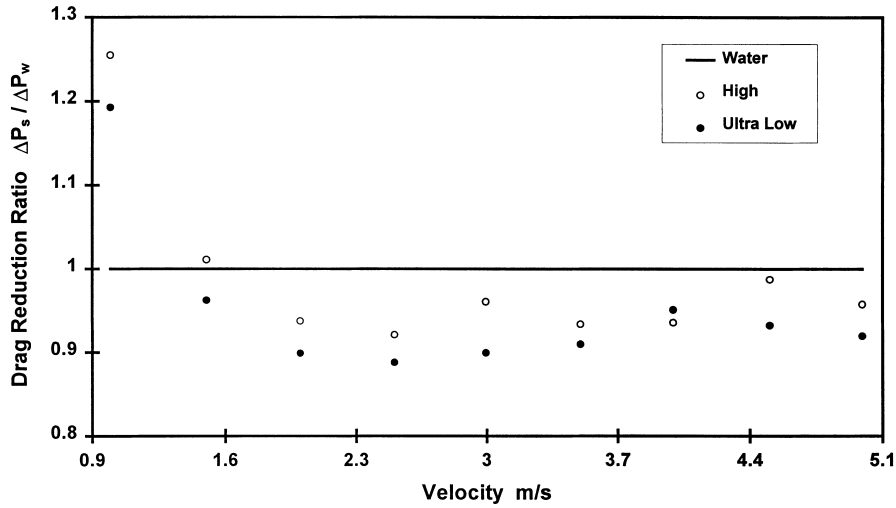

Fig. 8. Drag reduction ratio versus velocity for water and fibre suspension of 0.8% mass concentration. Bulk Temperature at 30°C and surface to bulk temperature difference as 5°C.

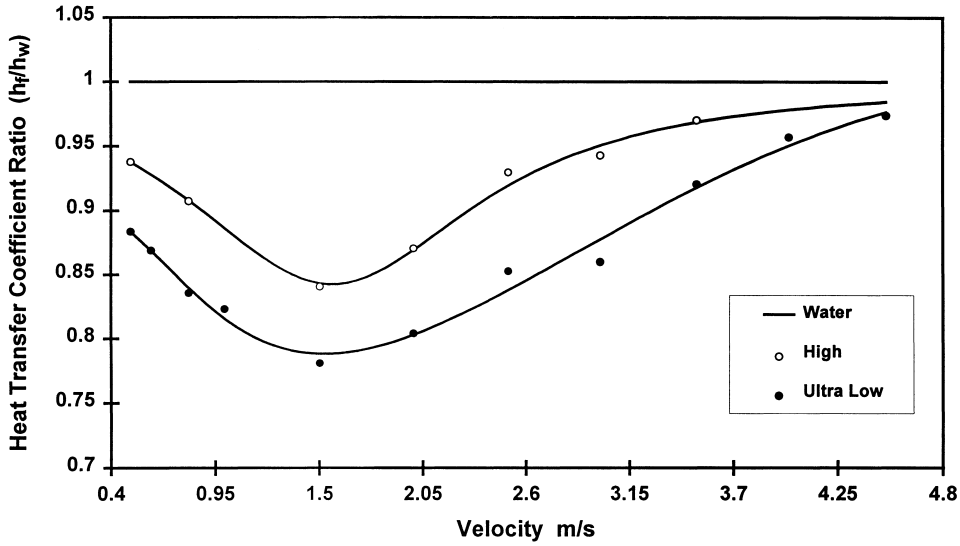

Fig. 9. Heat transfer coefficient ratio as a function of velocity for *Pinus Radiata* ultra low coarseness and high coarseness fibre suspensions in water at mass concentration 0.8 percent. Bulk temperature at 30°C and surface to bulk temperature difference as 5°C.

of the fibres in suspension. The measurement of heat transfer coefficient provides a new way to monitor wood pulp quality through fibre flexibility.

5. List of symbols

ε	roughness height,
r	radius of the circular duct,
ε/r	relative roughness,
V_m	average velocity,
f	friction factor (Fanning),
h	heat transfer coefficient,
Re	VD/v;
v	kinematic viscosity,
Nu	Nusselt number,
Pr	Prandtl number,
h_s	heat transfer coefficient of fibre suspension,
h_w	heat transfer coefficient of water,
ΔP_s	pressure drop in fibre suspensions,
ΔP_w	pressure drop in water
j_H	heat transfer j factor

References

[1] G.G. Duffy, A.L. Titchener, P.F.W. Lee, K. Moller, The mechanisms of flow of pulp suspensions in pipes, Appita 29(5) (1976) 363–370.
[2] G.G. Duffy, P.F.W. Lee, Drag reduction in the turbulent flow of wood pulp suspensions, Appita 31(4) (1978) 280–286.
[3] O. Reynolds, Scientific Papers 1, Cambridge University Press.
[4] N. Epstein, Monitoring Fouling, Proceedings of Fouling in Heat Exchangers Course, University of Auckland, New Zealand, February 1988, pp. 5.1-5.35.
[5] E.E. Wilson, A basis for the rational design of heat transfer apparatus, Trans. ASME 37(47) (1915) 47–82.
[6] C.F. Colebrook, Turbulent flow in pipes with particular reference to the transition region between the smooth and rough pipe laws, J. Inst. Civ. Eng. 11 (1939) 133–156.
[7] R.C. Martinelli, Heat transfer to molten metals, Trans. ASME 69 (1947) 947–959.
[8] G.G. Duffy, A Study of the Flow Properties of New Zealand Wood Pulp Suspensions, Ph.D. Thesis, Department of Chemical and Materials Engineering, The University of Auckland, Auckland, 1972.
[9] H. Hausen, Darstellung des Warmeuberganges in Rohren durch Verallgemeinerte Potenzbeziehungen, Z. Ver. Dtsch. Ing., Beiheft Verfahrenstechnik 4 (1943) 91–134.
[10] B.R. Bird, E.W. Stewart, N.E. Lightfoot, Transport Phenomena, Chapter 13, Wiley, New York, 1960.